AGU PUBLICATIONS

JGR

Journal of Geophysical Research: Space Physics

RESEARCH ARTICLE
10.1002/2016JA023526

Key Points:
- Two magnetic flux ropes were observed in tailward high-speed flows
- The two flux ropes were confirmed to be coalescing
- A basic criterion for identifying the coalescence is provided

Correspondence to:
R. Wang and Q. Lu,
rswan@ustc.edu.cn; qmlu@ustc.edu.cn

Citation:
Zhao, Y., R. Wang, Q. Lu, A. Du, Z. Yao, and M. Wu (2016), Coalescence of magnetic flux ropes observed in the tailward high-speed flows, *J. Geophys. Res. Space Physics*, *121*, 10,898–10,909, doi:10.1002/2016JA023526.

Received 28 SEP 2016
Accepted 24 OCT 2016
Accepted article online 27 OCT 2016
Published online 12 NOV 2016

Coalescence of magnetic flux ropes observed in the tailward high-speed flows

Yan Zhao[1,2], Rongsheng Wang[3], Quanming Lu[3], Aimin Du[1], Zhonghua Yao[1,4], and Mingyu Wu[3]

[1]Key Laboratory of Earth and Planetary Physics, Institute of Geology and Geophysics, Chinese Academy of Sciences, Beijing, China, [2]University of Chinese Academy of Sciences, Beijing, China, [3]CAS Key Laboratory of Geospace Environment, Department of Geophysics and Planetary Science, University of Science and Technology of China, Hefei, China, [4]Mullard Space Science Laboratory, University College London, Dorking, UK

Abstract We report a tailward high-speed flow event observed by Cluster during 0203:00UT–0205:30UT on 20 September 2003. Within the flows, a series of three bipolar B_z signatures were observed. The first and third bipolar B_z signatures are identified as magnetic flux ropes, while the middle one is found to result from the collision of the two flux ropes. A vertical thin current layer was embedded in the center of the middle bipolar B_z signature. Combining the plasma, electric field, and wave data around the thin current layer, we conclude that the two magnetic flux ropes were coalescing. The observations indicate that coalescence of magnetic flux ropes can happen in the regions away from reconnection site and can produce energetic electrons and waves. A basic criterion for identifying the coalescence in the magnetotail is proposed also.

1. Introduction

Magnetic flux ropes are a kind of helical magnetic structure consisting of a strong core field at their centers. They are frequently observed within the current sheets on the magnetopause [*Russell and Elphic*, 1978; *Rijnbeek et al*., 1984; *Scholer*, 1988; *Wang et al*., 2006; *Teh et al*., 2010] and in the magnetotail [e.g., *Moldwin and Hughes*, 1991; *Slavin et al*., 2003; *Walsh et al*., 2007; *Wang et al*., 2012; *Zhao et al*., 2016]. In the magnetotail, the current sheet is sandwiched between the magnetic field lines directed sunward in the Northern Hemisphere and the magnetic field lines directed antisunward in the Southern Hemisphere, and therefore its current directs mainly to the duskside. As a result, the typical signatures of the flux ropes are a south-then-north variation of magnetic field in the earthward flows or a north-then-south variation of magnetic field in the tailward flows, associated with a core field along the current direction.

Magnetic flux ropes play an important role in the process of magnetic reconnection [*Drake et al*., 2006; *Fu et al*., 2006; *Chen et al*., 2008; *Lu et al*., 2013; *Wang et al*., 2016]. The simulations show that flux ropes can enhance the reconnection rate [*Daughton et al*., 2006; *Huang et al*., 2011] and accelerate electrons [*Drake et al*., 2006; *Fu et al*., 2006; *Chen et al*., 2008; *Wang et al*., 2010]. Recently, the interaction of magnetic flux ropes was thought to be crucial for the evolution of magnetic reconnection itself [*Daughton et al*., 2011]. The coalescence of magnetic flux ropes has been simulated [*Finn and Kaw*, 1977; *Biskamp and Welter*, 1980; *Pritchett*, 2008; *Oka et al*., 2010; *Cazzola et al*., 2015]. During the coalescence of two flux ropes, a thin current sheet can be formed between their interaction regions. Therefore, the magnetic field lines of the two flux ropes can reconnect. Although the coalescence of magnetic flux ropes has been extensively studied by both theories and simulations [*Finn and Kaw*, 1977; *Biskamp and Welter*, 1980; *Pritchett*, 2008; *Oka et al*., 2010; *Zhou et al*., 2014; *Cazzola et al*., 2015], in situ evidence has not been reported until recently by *Wang et al*. [2016]. In *Wang et al*. [2016], the coalescence was observed inside the ion diffusion region and was regarded to be an integral part of magnetic reconnection. With the Magnetospheric Multiscale Mission (MMS) data at the magnetopause, *Øieroset et al*. [2016] reported an ion jet within a large flux rope and suggested that it could be the result of the coalescence. So far, many questions on the coalescence remain, e.g., whether the coalescence can occur in the region away from the reconnection site and how long the coalescence can proceed.

Here we report a Cluster observation of a potential coalescence event in the tailward high-speed flows. In the tailward flows, a vertical thin current layer was embedded in a south-then-north magnetic field signature which could have resulted from the collision of two flux ropes moving tailward. Moreover, a basic criterion is suggested to identify the coalescence event in the magnetotail.

2. Data

The data used in this paper are obtained from several instruments on board Cluster. The magnetic field data with time resolution of 1/22 s are taken from the Fluxgate Magnetometer (FGM) experiment [*Balogh et al*., 2001]. The plasma data are obtained from the Cluster Ion Spectrometry (CIS) experiment which consists of a Hot Ion Analyser and ion Composition and Distribution Function analyzer (CODIF) [*Rème et al*., 2001], and only the proton data with time resolution of 8 s from CODIF instrument are used here. The electric field and spacecraft potential data, with time resolutions of 0.04 s and 0.2 s, respectively, are obtained from the Electric Field and Wave (EFW) instrument [*Gustafsson et al*., 2001]. The spacecraft potential in this paper is used to derive electron density [*Pedersen et al*., 2008]. The electron data with 4 s resolution are obtained from High Energy Electron Analyser (HEEA) which is part of the Plasma Electron and Current Experiment (PEACE) instrument [*Johnstone*, 1997]. The data of electric and magnetic wave spectrograms with time resolution of 1 s are from Spatio Temporal Analysis of Field Fluctuations (STAFF) experiment [*Cornilleau-Wehrlin et al*., 1997]. If not specified, the GSM coordinate system (the geocentric solar magnetospheric coordinate system in which the x axis directs from the Earth to the Sun; the z axis, lying in the plane containing the x axis and the Earth's magnetic dipole, is perpendicular to the x axis and points north; and the y axis completes the right-handed coordinate system) is used in this paper.

3. Observations

Figure 1 displays an overview of the observations during 0203:00 UT to 0205:30 UT on 20 September 2003, when Cluster was situated in [−18.0, 4.0, −1.4] R_E. From 0203:00 UT to 0204:54 UT, Cluster observed the tailward high-speed flows and its speeds gradually increased from about 300 km/s to 900 km/s (Figure 1a). Afterward, the flow velocity quickly reduced to below 200 km/s. Inside the flows, the ion plasma beta values were mainly larger than 1 (Figure 1a, the blue dashed curve) and the B_x component of the magnetic field was smaller than 10 nT (Figure 1c). It indicates that the spacecraft was in the inner plasma sheet [*Baumjohann et al*., 1989; *Boakes et al*., 2014]. The energy of the ions exceeded the limit of the energy maximum of the CIS (~40 keV, Figure 1h) which further indicates that the spacecraft crossed the center of the plasma sheet.

Within the high-speed flows, at least three bipolar B_z signatures were observed (Figure 1e), and their reversal points were at 0203:30 UT, 0204:22 UT, and 020437 UT, respectively. As for the first and the third ones (marked by the yellow horizontal bars in Figure 1e), B_z varied from northward ($B_z > 0$) to southward ($B_z < 0$), and the magnetic field magnitudes were both enhanced (Figure 1f). Thus, we concluded that the first and third bipolar B_z signatures correspond to magnetic flux ropes moving tailward, called FR1 and FR2. Inside the flux rope FR1, there was a clear core field pointing to the duskside (Figure 1d). In contrast, there was no significant enhancement of B_y inside the FR2 where B_y was negative (dawnward) near its center and positive (duskward) at its boundary regions. The minimum variance analysis (MVA) [*Sonnerup and Cahill*, 1968] is applied to the magnetic field of two flux ropes to confirm their axis directions. The axis of FR1 was [−0.38, 0.89, −0.24] GSM and didn't lie exactly in the x-y plane, which may be the reason that the peak of B_y was not at the point where $B_z = 0$. As for the FR2, the MVA result depends on the chosen interval. It indicates that its inner core field is complex. Since the two flux ropes were observed by all four satellites, the timing method [*Henderson et al*., 2006] can be used to estimate their velocities. In order to evaluate the FR1 and FR2 velocities, the timing method was performed on the magnetic field B_y within them. The velocities for FR1 and FR2 were [−350, − 62, − 24] km/s and [−627, − 110, − 44] km/s, respectively, consistent with the plasma bulk flow speeds.

The two flux ropes were both propagating tailward but with different velocities. The FR1 was in the farther tailward of the FR2, as shown in Figure 2. The speed of FR2 is much higher than FR1 in the x direction. In other words, the FR2 was approaching the FR1. Between the two flux ropes, there was another bipolar B_z signature at ~0204:22 UT. In contrast to the FR1 and FR2, the B_z signature at ~0204:22 UT varied from southward ($B_z < 0$) to northward ($B_z > 0$) in association with a significant enhancement of B_y, directed to the dawnward. Corresponding to the enhancement of B_y, the electron density shows a dip (Figure 1b). Apparently, this south-then-north bipolar B_z signature cannot be attributed to a tailward moving magnetic flux rope, although it was detected in the tailward high-speed flows. In order to further understand this unexpected bipolar signature between FR1 and FR2, the data in the shaded area was enlarged in Figure 3.

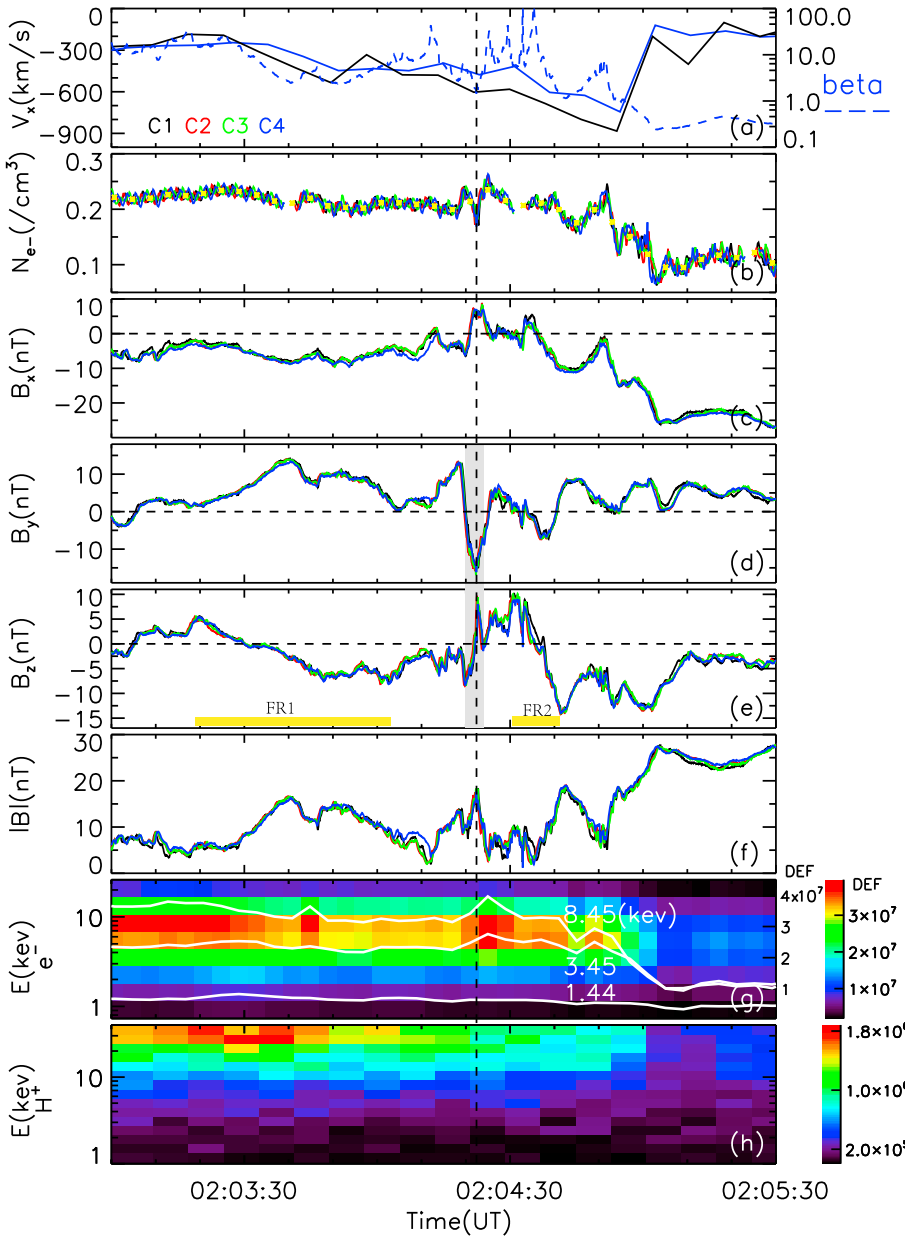

Figure 1. Cluster measurements during the interval 0203:00–0205:30UT on 20 September 2003. (a) The *x* component proton bulk flow (the solid lines) and the ion plasma beta values (the blue dashed lines), (b) the electron density derived from the electric potential (the four colored curves with a color scheme of black, red, green and blue for spacecraft 1–4) and that obtained by PEACE on board C2 (the yellow asterisk-dotted line), (c–f) three components and magnitude of the magnetic field, (g) the electron differential energy flux (DEF) spectrogram in the range 0.7 keV to 26 keV from spacecraft C2, and (h) the proton DEF spectrogram in the range 1 keV to 40 keV from spacecraft C4. The shaded region in Figure 1e represents the unexpected bipolar B_z (the interval showed in Figure 3). The two yellow bars in the bottom of Figure 1e denote the two flux ropes FR1 and FR2. The vertical black dashed line is the same with that in Figure 3, denoting the J_y peak calculated by curlometer technique. The three white curves in Figure 1g represent the energy flux of electrons with energies of 1.44, 3.45, and 8.45 keV.

From top to bottom, Figure 3 shows two components of the electric field in ISR2 coordinates (the Inverted SR2 coordinate system in which the *x* axis is in the meridian containing the direction of the Sun; the *z* axis, aligned with the maximum principal inertia axis of the spacecraft, is perpendicular to the *x* axis and points north; and the *y* axis completes the right-handed coordinate system.), three components of the magnetic field, the current density estimated from Curlometer technique, *y* and *z* components of the current density

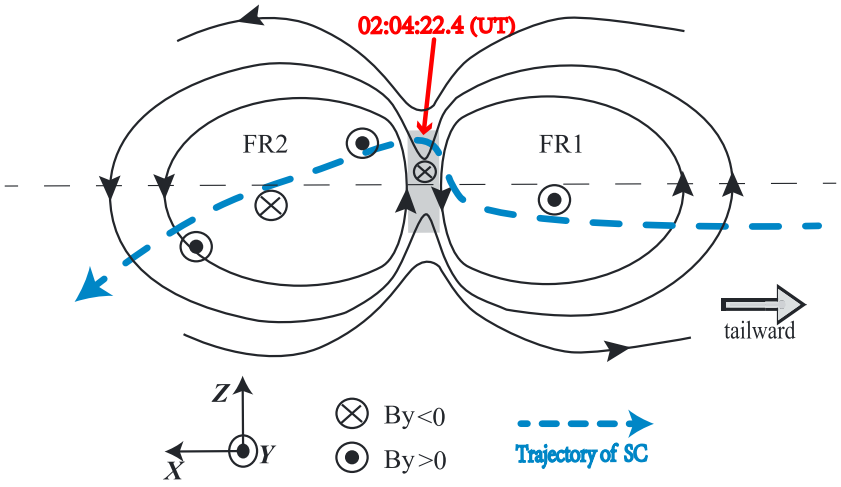

Figure 2. The illustration of coalescence of flux ropes in the *x-z* plane. The black arrowed lines denote the magnetic field lines of emerging flux ropes. The blue thick line denotes the trajectory of the spacecraft passing through the merging region. The red arrowed line denotes the time when the electric current peaks and the electron density dip were observed. The shaded region denotes the coalescence region.

derived from the magnetic field at a single satellite, and errors for the Curlometer technique during the unexpected bipolar B_z at about 0204:22 UT. The B_z component (Figure 3e) first decreased from about −1 nT at 0204:19.00 UT to −8 nT at 0204:19.75 UT, then increased to about 10 nT at about 0204:22.50 UT within 3 s, and later decreased to 0 at 0204:23.50 UT. At the same time, B_y gradually increased and peaked at the reversal point of B_z (Figure 3d). Also, the velocity of such unexpected bipolar B_z signature can be evaluated by the timing method. The estimated velocity was [−522, − 92, − 36] km/s, basically consistent with the tailward ion bulk flows. Therefore, this unexpected bipolar B_z signature cannot be a magnetic flux rope moving tailward. The Curlometer technique [*Dunlop et al*., 2002] was applied to estimate the current density around the signature, shown in Figure 3f. By treating the current as constant over the separation of the four spacecraft, we can estimate the current density from Ampere's law using the magnetic field alone at the four points [*Dunlop et al*., 2002]. It is clear that a substantial enhancement of j_y can be found near the center of the unexpected signature at ~ 0204:22 UT. The parameter j_y can reach ~ −40 nA/m^2 and is pointed to the dawnside, contrary to the current sheet in the magnetotail where the currents are mainly directed to the duskside. The normal direction of this thin current layer was estimated to be [0.92, −0.08, −0.38] by the MVA analysis [*Sonnerup and Cahill*, 1968], and thus its normal direction was mainly in the *x* direction. Namely, this current layer was lying in the *y-z* plane, perpendicular to the current sheet in the magnetotail.

The duration of the thin current layer was about 0.5 s, comparable to the time lags of $B_z = 0$ at the four satellites (Figure 3e). It indicates that its thickness was less than the separation of the spacecraft. So the current density is underestimated from the Curlometer technique [*Dunlop et al*., 2002]. During the interval while Cluster crossed the vertical current layer (around 0204:22 in Figure 3), B_x is nearly constant. Moreover, the current layer was mainly in the *y-z* plane. Therefore, the current density can be roughly estimated by $j_y \approx (\partial B_z/\partial x)/\mu_0$ and $j_z \approx -(\partial B_y/\partial x)/\mu_0$ at each single satellite, assuming that the time evolution is due to the spatial motion. The results at C2 and C4 are shown in Figure 3g to compare the electric field data in higher resolution available also at C2 and C4. A dawnward current layer was evident near the B_z reversal points at each satellite; its value can be up to −80 nA/m^2 and its duration was only about 0.2 s. The thickness of this current layer was ~ 104 km in the *x* direction, about 8.6 d_e (d_e: electron inertial length, ~12 km for $N_e = 0.2$ cm^{-3}), much smaller than the ion gyroradius (~1000 km, for protons with energy of 10 keV). So this current layer should be formed by the electrons, as previously reported [*Nagai et al*., 2011, 2013; *Petrukovich et al*., 2015].

A thin current layer was observed between two flux ropes moving tailward. The current inside this current layer points to the dawnside and is sandwiched by the trailing part of the FR1 and the leading part of the FR2. This scenario is consistent with the coalescence of a pair of flux ropes [*Finn and Kaw*, 1977]. As the spacecraft retreated from the FR1, $|B_z|$ gradually decreased from 0204:00 to 0204:19 UT and then sharply enhanced (a valley) at 0204:20 UT. Two seconds later, a peak of B_z was observed just as the spacecraft was entering the

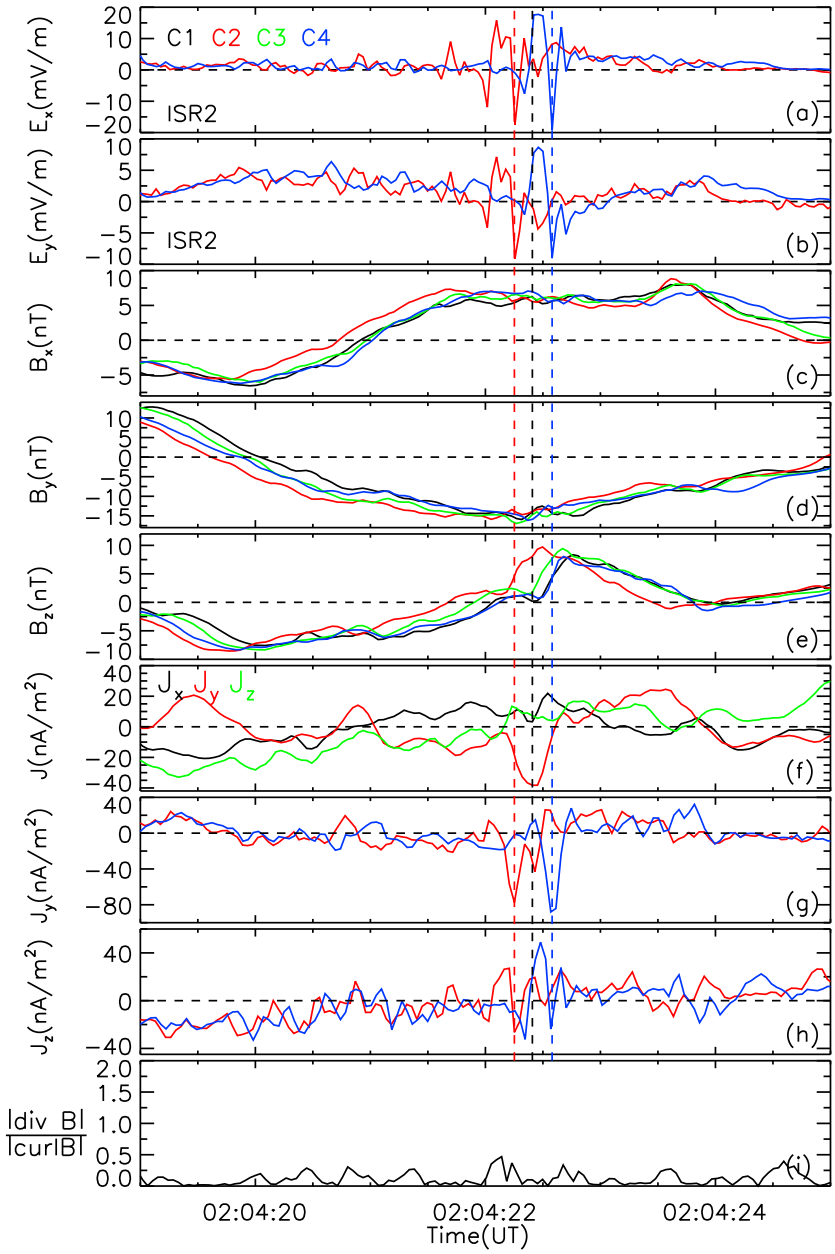

Figure 3. Expansion of the unexpected bipolar B_z. (a, b) The electric field E_x and E_y components in the ISR2 coordinate system and (c–e) three components of the magnetic field. The color code is the same as that in Figure 1. (f) The x (black), y (red), and z (green) components of the current density derived using the curlometer technique; (g, h) the J_y and J_z components of current density calculated using single-satellite data (red for C2 and blue for C4); and (i) the fractional error in the curlometer technique. The vertical black dashed line denotes the J_y peak calculated by curlometer technique, while the colored dashed lines denote the J_y peaks calculated using a single satellite.

FR2. Thus, it seems that the B_z component of magnetic field in the trailing part of the FR1 and in the leading part of the FR2 was compressed. The velocity estimation indeed supports this conclusion, since the velocity of FR2 (−627 km/s) was higher than that of FR1 (−350 km/s). The dawnward thin current layer was induced by the compressed magnetic field B_z. Whether the coalescence was occurring between these two flux ropes is still unclear.

The electric field fluctuated strongly (Figure 3a and b) at each satellite, while the satellite got into the surrounding region of the dawnward current layer (Figure 3g). Especially, E_y became the same direction (dawnward, $E_y < 0$) to J_y. It implies that magnetic energy might be dissipated in the thin current layer. Due

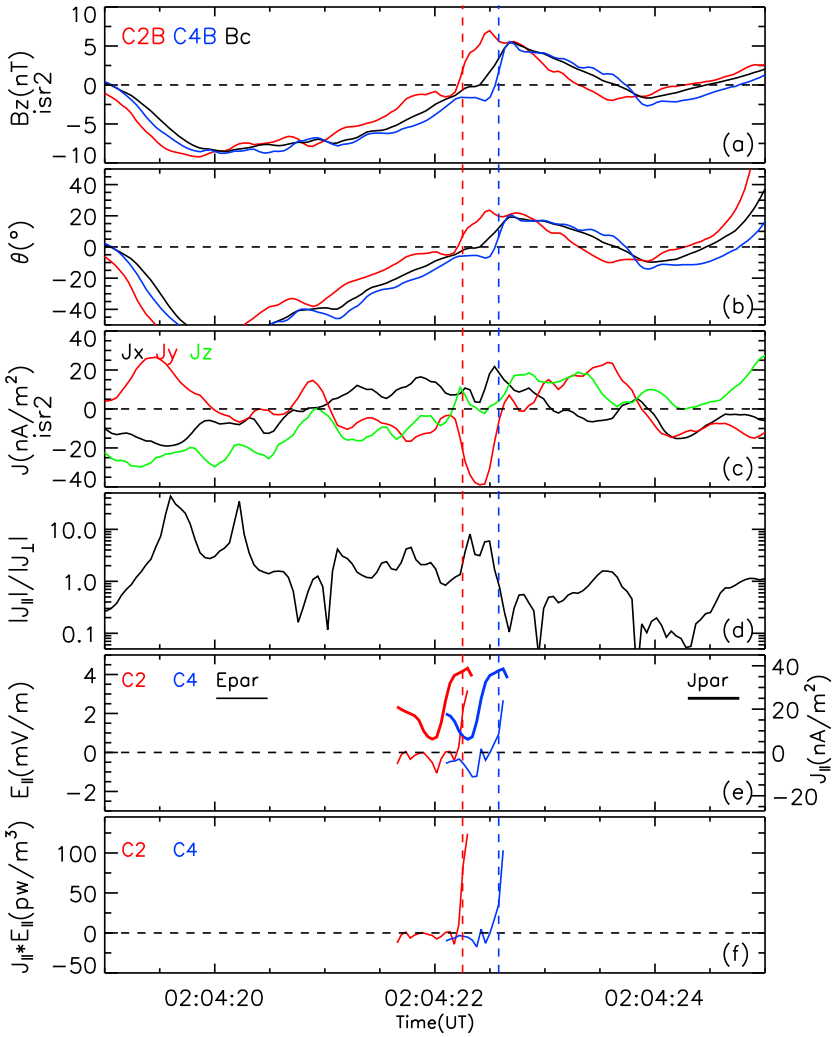

Figure 4. Quantities in in ISR2 coordinate system. (a) The B_z components of the magnetic field at C2 (red), C4 (blue), and the barycenter (black); (b) the inclination angles from the spin plane for the magnetic field at C2 (red), C4 (blue), and the barycenter (black); (c) the three components of the current density derived by curlometer technique; (d) the ratio of the parallel component to the perpendicular component of current density; (e) the parallel components of the electric field (thin lines) at C2 (red) and C4 (blue) in the spin plane and the parallel component of current density (thick lines) shifted to C2 (red) and C4 (blue); and (f) the joule heating $j_{||} \cdot E_{||}$ for C2 (red) and C4 (blue). Note that in Figures 4e and 4f, the parallel electric field, current density, and $j_{||} \cdot E_{||}$ are showed only when the magnetic inclination angle is less than 10°. The vertical colored dashed lines are the same with those in Figure 3.

to the lack of the electron velocity and the third component of the electric field, the energy dissipation quantity ($E \cdot J$) cannot be accurately obtained here. The ratio of $|j_{///}/j_{\perp}|$ is larger than 3 in the thin current layer during 0204:22.3–0204:22.5 (Figure 4d). Thus, the current density was mainly in the parallel direction (Figure 4d) in the current layer. It means that the energy dissipation quantity can be primarily from the parallel component ($j_{||} \cdot E_{||}$) in the vertical current layer. In order to estimate $j_{||} \cdot E_{||}$, we have to evaluate the parallel electric field and the parallel current at first. It is a challenging work to evaluate the parallel electric field by the Cluster measurement, because only two components of electric field in the spin plane are measured. Fortunately, the angle θ between the magnetic field and the spacecraft spin plane was close to 0 ($\theta < 10^o$) for a short while (0204:22.0–0204:22.6 for B_c) inside the thin current layer, as shown in Figure 4b. Then, the parallel electric field can be estimated in this short span and its values can reach 2.5 mV/m (Figure 4e). The parallel electric field can be estimated at a single satellite (C2 and C4) for the short span ($\theta < 10^o$), whereas the parallel current density cannot be obtained by the magnetic field at a single satellite. So the parallel current density from the Curlometer technique was used instead, which will cause the underestimation of $j_{||} \cdot E_{||}$. The results show

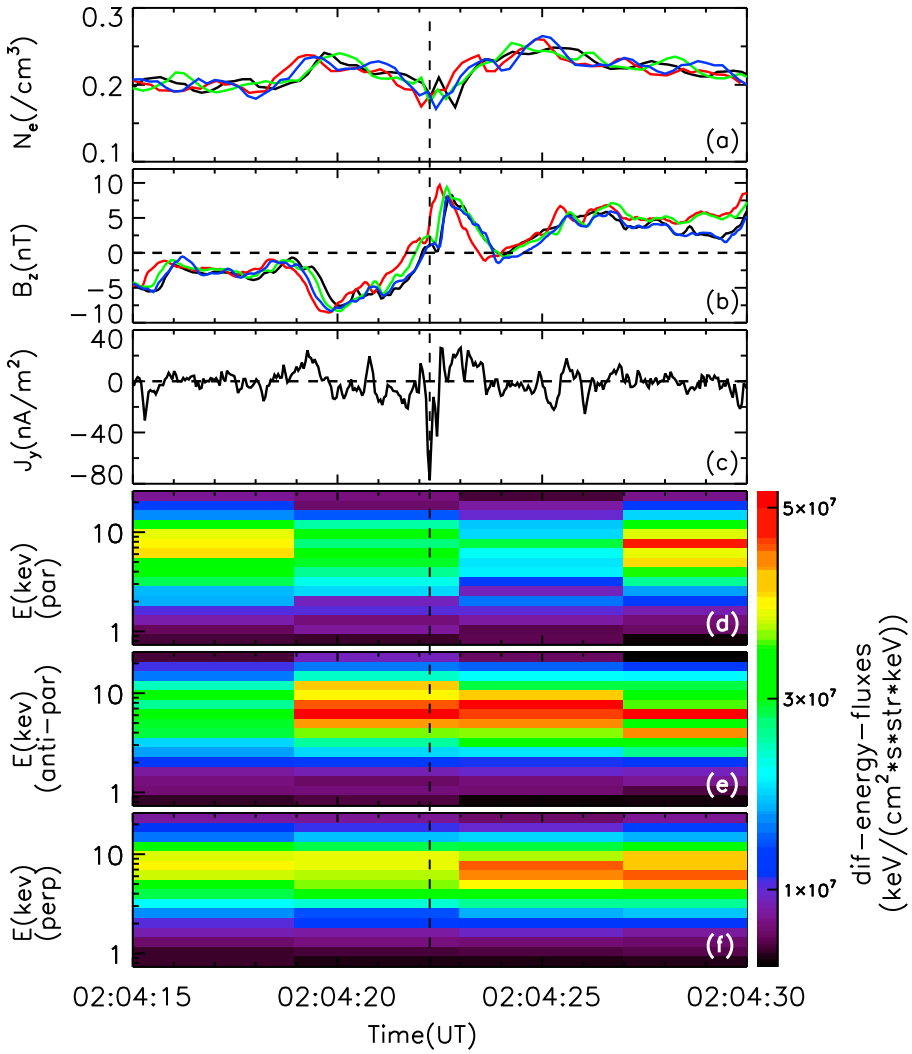

Figure 5. The electron differential energy fluxes around the coalescence current layer. (a) the electron density, (b) the B_z component of the magnetic field, (c) the J_y components of current density calculated using single-satellite data from C2, (d–f) The averaged electron differential energy fluxes in the parallel (0°–45°), antiparallel (135°–180°), and perpendicular directions (45°–135°), derived from the pitch angle data at C2.

that the $j_{\|} \cdot E_{\|}$ was positive (100 pW/m^3) inside the current layer (Figure 4f); i.e., the magnetic energy was releasing. The electron differential energy fluxes were enhanced (Figure 1g) while the spacecraft entered the thin current layer at 0204:22 UT. The fluxes between 3 keV and 8.5 keV display a localized peak near the center of the thin current layer (white traces in Figure 1g). It indicates that the electrons can be energized near the thin current layer. The electron differential energy fluxes in the parallel (0°~45°), antiparallel (135°~180°), and perpendicular directions (45°~135°) are displayed in Figures 5d–5f, respectively. The fluxes in the antiparallel direction are stronger than the other two directions. It means that the electrons were mainly accelerated in the direction antiparallel to the magnetic field. The previous observations do find that the electrons are mainly accelerated in the field-aligned direction around the reconnecting current sheet [e.g., *Wang et al.*, 2013; *Burch et al.*, 2016; *Chen et al.*, 2016].

The wave properties around the thin current layer are displayed in Figure 6. The electric field and magnetic field wave power spectral densities (PSD, from C2) between 0204:15 and 0204:30 UT are shown in Figures 6b and 6c. The vertical dashed line corresponds to the red vertical dashed line in Figure 3, denoting the peak of J_y at C2 (Figures 5c and 3g). It is evident that the waves are enhanced between the lower hybrid frequency (f_{LH}) and the electron cyclotron frequency (f_{ce}) in the thin current layer (Figures 6b and 6c). The electric field

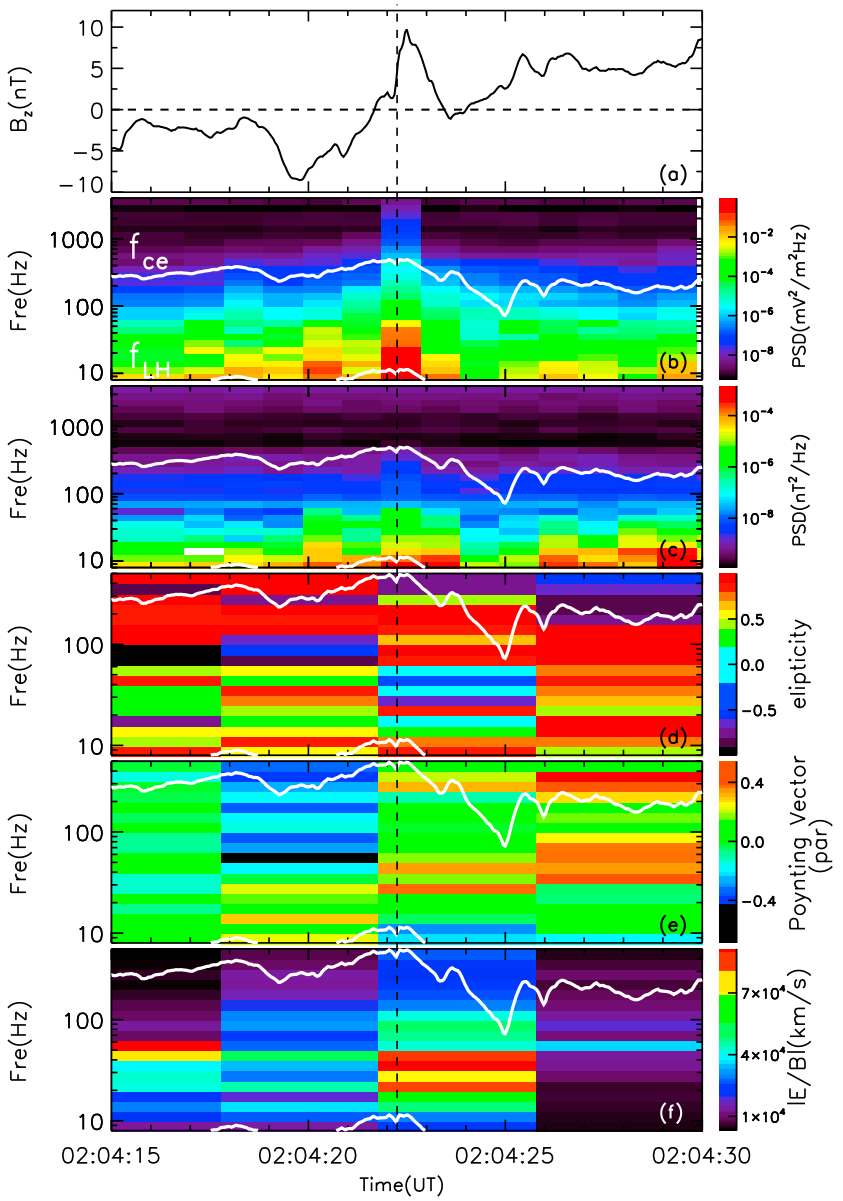

Figure 6. Wave properties around the coalescence current layer. (a) The B_z component of the magnetic field at C2, (b) electric field wave spectrogram with time resolution of 1 s in the range 8 Hz to 4 kHz, and (c) magnetic field wave spectrogram with time resolution of 1 s in the range 8 Hz to 4 kHz. (d) Wave ellipticity, (e) parallel component of the Poynting vector normalized by its standard deviation, and (f) the phase speed of waves estimated by $|E|/|B|$. Note that the time resolution of wave property data (Figures 6e and 6f) is 4 s. The wave data are from the STAFF experiment on board C2. The vertical dashed line is the same as that in Figure 5, denoting the J_y peak at C2.

fluctuations are broad bands and the strongest near the thin current layer. Figure 6d shows the ellipticity of these waves. Around the thin current layer (0204:18–0204:26 UT), the ellipticity is close to +1 above 60 Hz. Thus, the observed waves in the frequency range are right-hand circular polarization. It indicates that the observed waves can be electromagnetic whistler waves. In the same frequency range (60 Hz ~ f_{ce}), The parallel component of Poynting vector (Figure 6e) was negative before the thin current layer and became positive after the thin current layer. It means that the waves were propagating antiparallel to magnetic field before the thin current layer and changed to the direction parallel to magnetic field after the thin current layer. Considering the trajectory of the spacecraft shown in Figure 2, the waves were propagating away from the coalescing thin current layer. The phase speed of the waves can be estimated by $|E|/|B|$ and was about

2.4×10^4 km/s. The wave length along the magnetic field can be roughly estimated by $\lambda_{//} = v_{phase}/f$, to be 50 km. The wave properties are basically consistent with the previous observations [e.g., *Wei et al*., 2007; *Graham et al*., 2016]. Since the electric field was only measured in the two components within the spin plane, the power of the electric field is underestimated. The higher-frequency electrostatic waves will also cause the errors of the estimated phase speed.

4. Discussion and Summary

In this paper, we report a series of three bipolar B_z signatures within the tailward high-speed flows. We examined the plasma data 20 min after these flows and the continued tailward flows were observed without any earthward flows following, as shown in Figure 7b. It means that the bipolar B_z signatures (corresponding to the vertical dashed line in Figure 7) are away from a reconnection X line. The first (FR1) and third (FR2) bipolar signatures are identified as magnetic flux ropes moving tailward, while the second bipolar signature shows a south-then-north variation which cannot be a magnetic flux rope in the tailward flows. Further investigation finds that a thin current layer lying in the *y-z* plane is embedded near the center of this second bipolar signature. The current directs to the dawnward. More importantly, $E \cdot J$ was mainly from $j_{||} \cdot E_{||}$, and $j_{||} \cdot E_{||}$ is as large as 100 pw/m^3 in the vertical current layer. In addition, the strongly disturbed electric field was detected, and the energetic electrons were also observed in the current layer. This observation is consistent with the scenario of the coalescence of a pair of flux ropes which has been verified recently by *Wang et al*. [2016]. In *Wang et al*. [2016], the coalescence of magnetic flux ropes is detected in the ion diffusion region and can play an important role in the evolution of magnetic reconnection. In this paper, we report on a coalescence event in the tailward high-speed flows, away from the reconnection site. It means that the coalescence of magnetic flux ropes is not only occurring within the ion diffusion region but also in the regions away from the reconnection site, e.g., the high-speed flows which are very common in the magnetotail. The fact is that the evidence of the coalescence in the magnetotail is very rare. The reason for such discrepancy could be that the current layer resulting from the interaction of two flux ropes is too narrow (electron scale) to be discerned. On the other hand, the coalescence is generally caused by the collision between two flux ropes with different sizes [*Wang et al*., 2016]. The coalescence itself therefore is a driven asymmetric reconnection with a guide field (i.e., the core field of the flux ropes). In other words, the quadrupolar Hall magnetic field and the symmetric Hall electric field directed to the center of the coalescing current layer are distorted and even completely deformed. So no typical characteristic feature can be used to find the coalescence site. All of these could be the reasons for the rare reports on the coalescence of magnetic flux ropes. Here we provide basic criteria to recognize the coalescence event in the magnetotail.

Considering the situations in the magnetotail, the criteria for identify the coalescence event are provided: (1) two flux ropes which are approaching in the tailward flows or earthward flows are detected, (2) a south-then-north bipolar B_z signature in the tailward flows or a north-then-south bipolar B_z signature in the Earthward flows is observed between the two flux ropes, (3) there is a vertical thin current layer to the normal dawn-dusk current sheet within the bipolar B_z between the two flux ropes, (4) the current direction of the thin current layer directs to the dawnside, and (5) $(E + V_e \times B) \cdot J$ is positive in the current layer (V_e is the electron velocity). There are some additional evidences, like the Hall electric field and magnetic field and waves and energetic electrons around the current layer. We have to point out that any one of the above criteria alone cannot be sufficient condition for identifying the coalescence, e.g., the localized dawnward current is detected also in the magnetic decrease region ahead of dipolarization front [*Yao et al*., 2013] and simulated in the global hybrid simulation [*Lu et al*., 2016]. In the magnetotail, the unexpected bipolar signatures of B_z (south-then-north in the tailward flows or north-then-south in the earthward) are frequently observed, without the signatures of magnetic flux ropes before and after it. For example, the south-then-north B_z bipolar signatures are repeatedly measured in the tailward flows in Figure 7e (e.g., 0209:30–0213:30). This unexpected bipolar signature of B_z could be the result of the coalescence of a pair of magnetic flux ropes, but the spacecraft missed the two flux ropes.

The collision between flux ropes may be the reason for their coalescence. In this event, the flux rope FR2 had a larger speed than FR1 ahead of it and therefore collided with the FR1. This collision will naturally pile up the localized magnetic field in the *z* direction (Figures 1e and 3e) and form the vertical thin current layer. The substantial enhancement of B_y in the thin current layer indicated that the magnetic field was indeed compressed

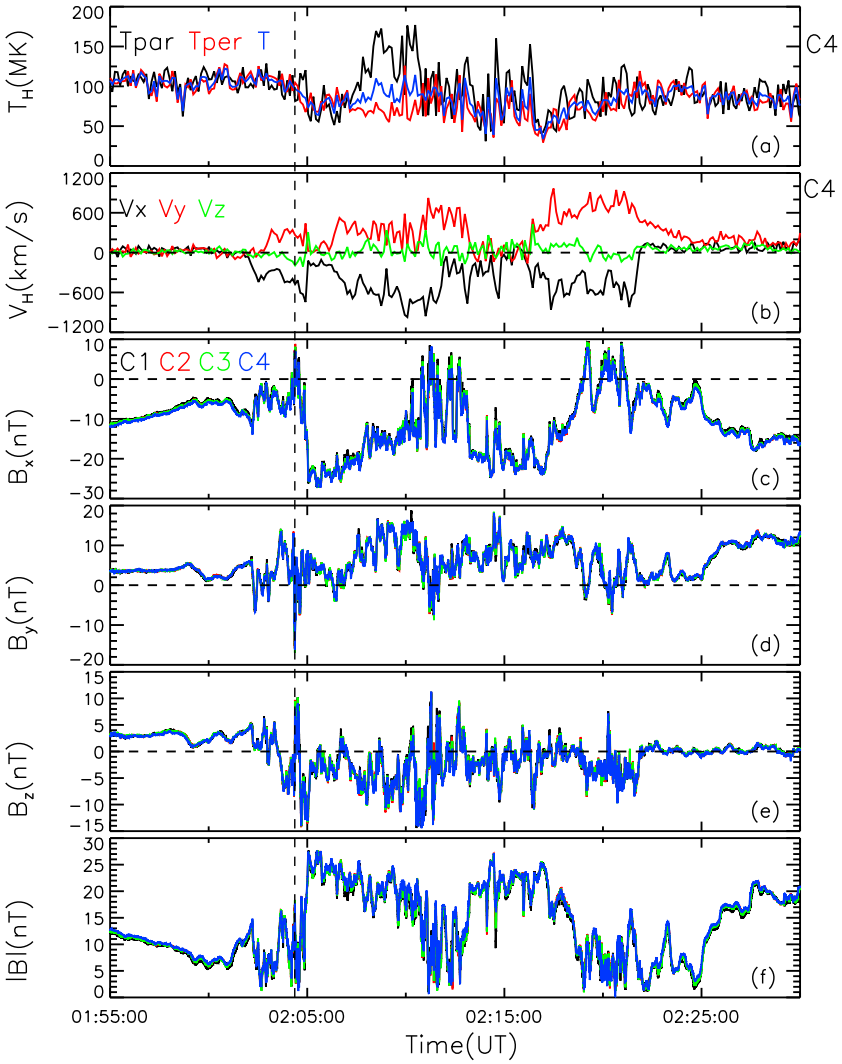

Figure 7. A longer time interval for the observations. (a) The parallel (black), perpendicular (red), and total temperature from C4, (b) the three components of proton bulk flow from C4, and (c–f) three components and magnitude of the magnetic field. The vertical dashed line denotes the time when the coalescence was observed.

(Figures 1d and 3d). Thus, the unexpected bipolar signature of B_z is a natural consequence of the collision of the two flux ropes. So far, there are still open questions whether the pileup of the magnetic field is necessary to trigger the coalescence and how long the coalescence can proceed in the magnetotail. At least, the magnetic field pileup was detected in the reported coalescence events in the magnetotail [*Wang et al.*, 2016] and also this event here. The energetic electrons and waves in the coalescing current layer indicate that the coalescence process could be similar to the normal reconnection in the magnetotail.

Generally, the plasma density is significantly enhanced in the center of flux ropes [e.g., *Khurana et al.*, 1995; *Chen et al.*, 2008; *Wang et al.*, 2016]. Thus, the occasionally observed density dip within a flux rope [*Retinò et al.*, 2008; and *Wang et al.*, 2010] is supposed to be caused by two coalescing flux ropes, as shown in the simulations [*Retinò et al.*, 2008; *Zhou et al.*, 2014]. However, if this dip is due to the coalescence, its spatial scale would be thereby comparable to the scales of the flux rope. In this observation, a density dip was indeed observed (Figures 1b and 5a). However, it was very short and only observed near the coalescing current layer (electron scale), which, apparently, wasn't consistent with the previous simulation result. The intense waves were observed around the coalescing current layer, and the identified whistler waves were propagating away from the coalescing current layer. The electrons are energized at the coalescing current layer. Thus, this density dip can be associated with the acceleration.

In conclusion, we report observations of a south-then-north bipolar B_z with strong core field in the tailward high-speed flows. By investigating the plasma and field data around the bipolar signature, we have now confirmed that the bipolar B_z corresponds to the coalescence of magnetic flux ropes. The observations indicate that coalescence of magnetic flux ropes can happen in high-speed flows away from the reconnection diffusion region. The criteria for identifying the coalescence event in the magnetotail are also suggested.

Acknowledgments
The authors wish to thank the Cluster Active Archive and Cluster instrument teams, in particular FGM, EFW, CIS, PEACE, and STAFF for providing the Cluster data which can be obtained at http://csa.esac.esa.int/csa/aio/html/home_main.shtml. This work is supported by the National Science Foundation of China (NSFC; grants 41674143, 41474126, 41331067, 41174122, 11220101002, and 41104092) and by the National Basic Research Program of China (2014CB845903 and 2013CBA01503).

References

Balogh, A., et al. (2001), The Cluster Magnetic Field Investigation: Overview of in-flight performance and initial results, *Ann. Geophys.*, *19*, 1207–1217, doi:10.5194/angeo-19-1207-2001.

Baumjohann, W., G. Paschmann, and C. A. Cattell (1989), Average plasma properties in the central plasma sheet, *J. Geophys. Res.*, *94*(A6), 6597–6606, doi:10.1029/JA094iA06p06597.

Biskamp, D., and H. Welter (1980), Coalescence of magnetic islands, *Phys. Rev. Lett.*, *44*, 1069, doi:10.1103/PhysRevLett.44.1069.

Boakes, P. D., R. Nakamura, M. Volwerk, and S. E. Milan (2014), ECLAT Cluster spacecraft magnetotail plasma region identifications (2001–2009), *Dataset Pap. Sci.*, *2014*, 684305, doi:10.1155/2014/684305.

Burch, J. L., et al. (2016), Electron-scale measurements of magnetic reconnection in space, *Science*, *352*(6290), aaf2939, doi:10.1126/science.aaf2939.

Cazzola, E., M. E. Innocenti, S. Markidis, M. V. Goldman, D. L. Newman, and G. Lapenta (2015), On the electron dynamics during island coalescence in asymmetric magnetic reconnection, *Phys. Plasmas*, *22*(9), 092901, doi:10.1063/1.4929847.

Chen, L. J., et al. (2008), Observation of energetic electrons within magnetic islands, *Nat. Physics*, *4*, 19–23, doi:10.1038/nphys777.

Chen, L.-J., et al. (2016), Electron energization and mixing observed by MMS in the vicinity of an electron diffusion region during magnetopause reconnection, *Geophys. Res. Lett.*, *43*, 6036–6043, doi:10.1002/2016GL069215.

Cornilleau-Wehrlin, N., et al. (1997), The CLUSTER Spatio-Temporal Analysis of Field Fluctuations (STAFF) experiment, *Space Sci. Rev.*, *79*, 107–136, doi:10.1007/978-94-011-5666-0_5.

Daughton, W., J. Scudder, and H. Karimabadi (2006), Fully kinetic simulations of undriven magnetic reconnection with open boundary conditions, *Phys. Plasmas*, *13*, 072101, doi:10.1063/1.2218817.

Daughton, W., V. Roytershteyn, H. Karimabadi, L. Yin, B. J. Albright, B. Bergen, and K. J. Bowers (2011), Role of electron physics in the development of turbulent magnetic reconnection in collisionless plasmas, *Nat. Phys.*, *7*, 539–542, doi:10.1038/nphys1965.

Drake, J. F., M. Swisdak, H. Che, and M. A. Shay (2006), Electron acceleration from contracting magnetic islands during reconnection, *Nature*, *443*, 553–556, doi:10.1038/nature05116.

Dunlop, M. W., A. Balogh, K.-H. Glassmeier, and P. Robert (2002), Four-point Cluster application of magnetic field analysis tools: The Curlometer, *J. Geophys. Res.*, *107*(A11), 1384, doi:10.1029/2001JA005088.

Finn, J. M., and P. K. Kaw (1977), Coalescence instability of magnetic islands, *Phys. Fluids*, *20*, 72, doi:10.1063/1.861709.

Fu, X. R., Q. M. Lu, and S. Wang (2006), The process of electron acceleration during collisionless magnetic reconnection, *Phys. Plasmas*, *13*, 012309, doi:10.1063/1.2164808.

Graham, D. B., A. Vaivads, Y. V. Khotyaintsev, and M. André (2016), Whistler emission in the separatrix regions of asymmetric magnetic reconnection, *J. Geophys. Res. Space Physics*, *121*, 1934–1954, doi:10.1002/2015JA021239.

Gustafsson, G., et al. (2001), First results of electric field and density observations by Cluster EFW based on initial months of operation, *Ann. Geophys.*, *19*, 1219–1240, doi:10.5194/angeo-19-1219.

Henderson, P. D., C. J. Owen, L. V. Alexeev, J. A. Slavin, A. N. Fazakerley, E. A. Lucek, and H. Rème (2006), Cluster observations of flux rope structures in the near-tail, *Ann. Geophys.*, *24*, 651–666, doi:10.5194/angeo-24-651-2006.

Huang, C., Q. M. Lu, Z. W. Yang, M. Y. Wu, Q. L. Dong, and S. Wang (2011), The evolution of electron current sheet and formation of secondary islands in guide field reconnection, *Nonlinear Processes Geophys.*, *18*, 727–733, doi:10.5194/npg-18-727-2011.

Johnstone, A. D. (1997), PEACE: A Plasma Electron and Current Experiment, *Space Sci. Rev.*, *79*, 351–398, doi:10.1023/A:1004938001388.

Khurana, K. K., M. G. Kivelson, L. A. Frank, and W. R. Paterson (1995), Observations of magnetic flux ropes and associated currents in the Earth's magnetotail with the Galileo spacecraft, *Geophys. Res. Lett.*, *22*, 2087–2090, doi:10.1029/95GL01518.

Lu, S., Q. Lu, C. Huang, and S. Wang (2013), The transfer between electron bulk kinetic energy and thermal energy in collisionless magnetic reconnection, *Phys. Plasmas*, *20*, 061203, doi:10.1063/1.4811119.

Lu, S., A. V. Artemyev, V. Angelopoulos, Q. Lu, and J. Liu (2016), On the current density reduction ahead of dipolarization fronts, *J. Geophys. Res. Space Physics*, *121*, 4269–4278, doi:10.1002/2016JA022754.

Moldwin, M. B., and W. J. Hughes (1991), Plasmoids as magnetic flux ropes, *J. Geophys. Res.*, *96*, 14,051–14,064, doi:10.1029/91JA01167.

Nagai, T., I. Shinohara, M. Fujimoto, A. Matsuoka, Y. Saito, and T. Mukai (2011), Construction of magnetic reconnection in the near-Earth magnetotail with Geotail, *J. Geophys. Res.*, *116*, A04222, doi:10.1029/2010JA016283.

Nagai, T., I. Shinohara, S. Zenitani, R. Nakamura, T. K. M. Nakamura, M. Fujimoto, Y. Saito, and T. Mukai (2013), Three-dimensional structure of magnetic reconnection in the magnetotail from Geotail observations, *J. Geophys. Res. Space Physics*, *118*, 1667–1678, doi:10.1002/jgra.50247.

Øieroset, M., et al. (2016), MMS observations of large guide field symmetric reconnection between colliding reconnection jets at the center of a magnetic flux rope at the magnetopause, *Geophys. Res. Lett.*, *43*, 5536–5544, doi:10.1002/2016GL069166.

Oka, M., M. Fujimoto, I. Shinohara, and T. D. Phan (2010), "Island surfing" mechanism of electron acceleration during magnetic reconnection, *J. Geophys. Res.*, *115*, A08223, doi:10.1029/2010JA015392.

Pedersen, A., et al. (2008), Electron density estimations derived from spacecraft potential measurements on Cluster in tenuous plasma regions, *J. Geophys. Res.*, *113*, A07S33, doi:10.1029/2007JA012636.

Petrukovich, A. A., A. V. Artemyev, I. Y. Vasko, R. Nakamura, and L. M. Zelenyi (2015), Current sheets in the Earth magnetotail: Plasma and magnetic field structure with Cluster project observations, *Space Sci. Rev.*, doi:10.1007/s11214-014-0126-7.

Pritchett, P. L. (2008), Energetic electron acceleration during multi-island coalescence, *Phys. Plasmas*, *15*, 102105, doi:10.1063/1.2996321.

Rème, H., et al. (2001), First multispacecraft ion measurements in and near the Earth's magnetosphere with the identical Cluster ion spectrometry (CIS) experiment, *Ann. Geophys.*, *19*, 1303–1354, doi:10.5194/angeo-19-1303-2001.

Retinò, A., et al. (2008), Cluster observations of energetic electrons and electromagnetic fields within a reconnecting thin current sheet in the Earth's magnetotail, *J. Geophys. Res.*, *113*, A12215, doi:10.1029/2008JA013511.

Rijnbeek, R. P., S. W. H. Cowley, D. J. Southwood, and C. T. Russell (1984), A survey of dayside flux transfer events observed by ISEE 1 and 2 magnetometers, *J. Geophys. Res.*, *89*, 786–800, doi:10.1029/JA089iA02p00786.

Russell, C. T., and R. C. Elphic (1978), Initial ISEE magnetometer results: Magnetopause observations, *Space Sci. Rev.*, *22*(6), 681–715, doi:10.1007/BF00212619.

Scholer, M. (1988), Strong core magnetic fields in magnetopause flux transfer events, *Geophys. Res. Lett.*, *15*, 748–751, doi:10.1029/GL015i008p00748.

Slavin, J. A., et al. (2003), Geotail observations of magnetic flux ropes in the plasma sheet, *J. Geophys. Res.*, *108*(A1), 1015, doi:10.1029/2002JA009557.

Sonnerup, B. U., and L. J. Cahill (1968), Explorer 12 observations of magnetopause current layer, *J. Geophys. Res.*, *73*, 1757–1770, doi:10.1029/JA073i005p01757.

Teh, W.-L., et al. (2010), THEMIS observations of a secondary magnetic island within the Hall electromagnetic field region at the magnetopause, *Geophys. Res. Lett.*, *37*, L21102, doi:10.1029/2010GL045056.

Walsh, A. P., A. N. Fazakerley, R. J. Wilson, I. V. Alexeev, P. D. Henderson, C. J. Owen, E. Lucek, C. Carr, and I. Dandouras (2007), Near-simultaneous magnetotail flux rope observations with Cluster and Double Star, *Ann. Geophys.*, *25*, 1887–1897, doi:10.5194/angeo-25-1887-2007.

Wang, R. S., et al. (2012), Asymmetry in the current sheet and secondary magnetic flux ropes during guide field magnetic reconnection, *J. Geophys. Res.*, *117*, A07223, doi:10.1029/2011ja017384.

Wang, R. S., et al. (2016), Coalescence of magnetic flux ropes in the ion diffusion region of magnetic reconnection, *Nat. Phys.*, doi:10.1038/nphys3578.

Wang, R., Q. Lu, X. Li, C. Huang, and S. Wang (2010), Observations of energetic electrons up to 200 keV associated with a secondary island near the center of an ion diffusion region: A Cluster case study, *J. Geophys. Res.*, *115*, A11201, doi:10.1029/2010JA015473.

Wang, R., A. Du, R. Nakamura, Q. Lu, Y. V. Khotyaintsev, M. Volwerk, T. Zhang, E. A. Kronberg, P. W. Daly, and A. N. Fazakerley (2013), Observation of multiple sub-cavities adjacent to single separatrix, *Geophys. Res. Lett.*, *40*, 2511–2517, doi:10.1002/grl.50537.

Wang, Y. L., R. C. Elphic, B. Lavraud, M. G. G. T. Taylor, J. Birn, C. T. Russell, J. Raeder, H. Kawano, and X. X. Zhang (2006), Dependence of flux transfer events on solar wind conditions from 3 years of Cluster observations, *J. Geophys. Res.*, *111*, A04224, doi:10.1029/2005JA011342.

Wei, X. H., J. B. Cao, G. C. Zhou, O. Santolík, H. Rème, I. Dandouras, N. Cornilleau-Wehrlin, E. Lucek, C. M. Carr, and A. Fazakerley (2007), Cluster observations of waves in the whistler frequency range associated with magnetic reconnection in the Earth's magnetotail, *J. Geophys. Res.*, *112*, A10225, doi:10.1029/2006JA011771.

Yao, Z. H., et al. (2013), Current structures associated with dipolarization fronts, *J. Geophys. Res. Space Physics*, *118*, 6980–6985, doi:10.1002/2013JA019290.

Zhao, Y., R. Wang, and A. Du (2016), Characteristics of field-aligned currents associated with magnetic flux ropes in the magnetotail: A statistical study, *J. Geophys. Res. Space Physics*, *120*, 3264–3277, doi:10.1002/2015JA022144.

Zhou, M., Y. Pang, X. Deng, S. Huang, and X. Lai (2014), Plasma physics of magnetic island coalescence during magnetic reconnection, *J. Geophys. Res. Space Physics*, *119*, 6177–6189, doi:10.1002/2013JA019483.